'94 KACC (1994. 10. 17 ~ 20)

Modeling and Vibration Control of High-Rise Buildings Using H_2 and H_∞ Control Theories

Minoru Hayase[1], Muhidin Arifin[2], Antonio Moran[1], Masayasu Shimakage[1]
(1) Tokyo University of Agriculture and Technology
Koganei-shi, Naka-cho, Tokyo 184, JAPAN
(2) Malaysian Technology Development Corporation
424 Jalan Tun Razak, Kuala Lumpur, MALAYSIA

Abstract

This paper analyzes the dynamical modeling of high-rise building and the design of control systems for suppressing undesired vibrational motion at the top of the building originated by natural disturbances such as earthquakes, wind, etc. The control system is designed according to H_2 and H_∞ robust control theories. The performance of the building with H_∞ controller is analyzed in the time and frequency domains and the vibration isolation and robustness properties of H_∞ and H_2 control systems are examined and compared. The design procedure, structure and properties of H_∞ controllers are analyzed.

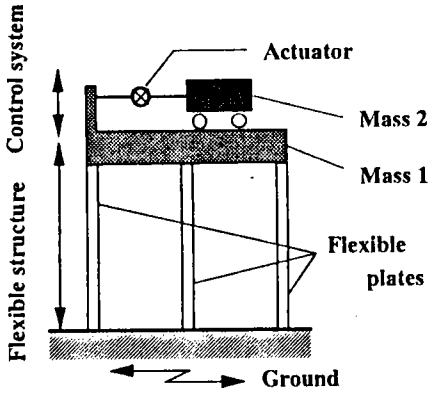

Figure 1: Fundamental structure of building model

1 Introduction

The trend of building construction in the near future will be of high-rise type. High-rise buildings have to be protected from natural disturbances such as earthquakes, wind forces, etc. This paper presents a design methodology of the control system to suppress undesired vibrational motion at the top of the building. The objective is to keep the lateral displacement of the top of the building as small as possible and to reduce the vibration transmissibility from ground motion (or wind forces) to the building compartments in order to reduce the vibration sensitivity of people staying inside the building as well as to reduce the vibrational stress of the building itself.

The structure of the building and control system are modeled as a 2 degrees-of-freedom system with spring, damper and lumped masses. The control system is designed according to H_2 and H_∞ control theories. According to these theories a controller is designed to minimize the energy transfer from disturbances $\mathbf{w}$ to controlled output variables $\mathbf{z}$. The amount of energy transfer is expressed by the norm (H_2 or H_∞) of the transfer function from $\mathbf{w}$ to $\mathbf{z}$.

The paper is organized as follows. Section 2 presents the dynamical modeling of the building including the determination of the state variables, measured output variables and controlled variables. Section 3 describes the generalized plant as well as the assumptions imposed on it. Section 4 details the procedure to design H_∞ controllers and analyzes their internal structure. Section 5 analyzes the frequency, step and random responses of the performance variables of the closed-loop system with H_∞ and H_2 controllers. Also the robustness properties of the closed-system and the estimation capabilities of H_∞ and H_2 observers are examined. Section 6 contains some concluding remarks.

2 Modeling of High-Rise Building

2.1 Motion equations

The fundamental structure of a high rise building and its control system are shown in Fig.1. The structure of the building may vibrate excited by ground motion (earthquakes) or lateral forces (wind). The control system is basically composed of an actuator and a vibrating mass. This mass vibrates driven by actuator forces which are properly regulated so that the actuator-mass structure of the control system absorbes the undesired vibrations of the building.

The building and control system can be modeled as a two degrees-of-freedom mass-spring-damper system as shown in Fig.2. In this figure m_1 represents the equivalent mass of the building and m_2 represents the mass of the vibrating body of the control system. Mass m_1 is connected to ground through a spring and damper connected in parallel. Masses m_1 and m_2 are connected by a spring and damper and a controlled actuator which provides regulated forces.

The equations describing the lateral motion of the

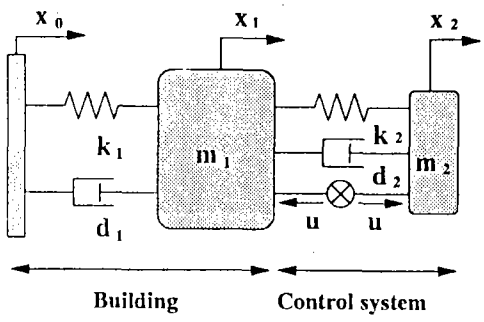

Figure 2: Two-degrees-of-freedom building model

building mass m_1 and vibrating mass m_2 are:

$$m_1\ddot{x}_1 = -k_1x_{10} - d_1\dot{x}_{10} + k_2x_{21} + d_2\dot{x}_{21} - u \quad (1)$$
$$m_2\ddot{x}_2 = -k_2x_{21} - d_2\dot{x}_{21} + u \quad (2)$$

where k_1, k_2 are spring constants, d_1 and d_2 are damping coefficients and u is the controlled force provided by the actuator whose dynamics is not considered. x_1 and x_2 are the absolute displacements of masses m_1 and m_2, respectively. x_{10} and x_{21} represent relative displacements: $x_{10} = x_1 - x_0$ and $x_{21} = x_2 - x_1$.

Defining the state vector $\mathbf{x}$

$$\mathbf{x} = [\,\dot{x}_2, \quad x_{21}, \quad \dot{x}_1, \quad x_{10}\,]^T \quad (3)$$

and combining Eqs.1 and 2, the following state-space equation can be formulated:

$$\dot{\mathbf{x}} = -\mathbf{A}\mathbf{x} + \mathbf{B}u + \mathbf{W}\omega_1 \quad (4)$$

where $\omega_1 = \dot{x}_0$. Matrices $\mathbf{A}$, $\mathbf{B}$ and $\mathbf{W}$ are:

$$\mathbf{A} = \begin{bmatrix} d_2/m_2 & k_2/m_2 & -d_2m_2 & 0 \\ -1 & 0 & 1 & 0 \\ -d_2/m_1 & -k_2/m_1 & (d_1+d_2)/m_1 & k_1/m_1 \\ 0 & 0 & -1 & 0 \end{bmatrix} \quad (5)$$

$$\mathbf{B} = \begin{bmatrix} 1/m_2 \\ 0 \\ -1/m_1 \\ 0 \end{bmatrix} \qquad \mathbf{W} = \begin{bmatrix} 0 \\ 0 \\ d_1/m_1 \\ -1 \end{bmatrix} \quad (6)$$

2.2 Measured output equation

Although several sensors can be used to measure the present value of the state variables of the building and its control system, in this paper it is assumed that an accelerometer measuring $\ddot{x}_1$ and a gap sensor measuring the relative displacement x_{21} are available. Since $\ddot{x}_1$ is not a state variable, it will be integrated to obtain the velocity $\dot{x}_1$ which together with x_{21} are the measured output variables. Considering the presence of measurement noise, the measured output vector $\mathbf{y}$ is:

$$\mathbf{y} = \begin{bmatrix} x_{21} + \omega_2 \\ \dot{x}_1 + \omega_3 \end{bmatrix} \quad (7)$$

where ω_2 and ω_3 represent the measurement noise.

2.3 Controlled Variables

The objective of the control system is to reduce the vibration of the building in order to minimize its mechanical stress as well as to reduce the vibration transmissibility to people staying inside the building. Several state variables may be selected as measure of the vibration of the building as well as measure of the performance of the control system: (a) acceleration of building mass $\ddot{x}_1$ is usually related to human sensitivity to vibrations and dynamical stress of building materials, (b) relative displacement of building components x_{10} is usually related to static stress of building materials. It is desirable that both variables be kept as small as possible.

Since both variables $\ddot{x}_1$ and x_{10} are directly related to the velocity of the building mass $\dot{x}_1$, in this paper $\dot{x}_1$ will be the performance variable to be minimized by the control system. Also, since the displacement of the vibrating mass of the control system x_{21} should be bounded and the control resources u are limited, both variables should also be kept at physically reasonable values. Therefore, the controlled variables of the system are chosen to be:

$$[\,u, \quad x_{21}, \quad \dot{x}_1\,]^T \quad (8)$$

3 Generalized Plant

By properly arranging the state-space equation, measured output equation and controlled variables, the *generalized plant* of the controlled system can be formulated as:

$$\dot{\mathbf{x}} = -\mathbf{A}\mathbf{x} + \mathbf{B}_1u + \mathbf{B}_2\mathbf{w} \quad (9)$$
$$\mathbf{y} = \mathbf{C}_1\mathbf{x} + \mathbf{D}_{11}u + \mathbf{D}_{12}\mathbf{w} \quad (10)$$
$$\mathbf{z} = \mathbf{C}_2\mathbf{x} + \mathbf{D}_{21}u + \mathbf{D}_{22}\mathbf{w} \quad (11)$$

where $\mathbf{z}$ represents the controlled vector composed of the controlled variables affected by weighting coefficients (c_2 and c_3) selected so that the closed-loop system meets the specifications. $\mathbf{w}$ represents the disturbance vector composed of plant disturbances and measurement noise:

$$\mathbf{z} = \begin{bmatrix} u \\ c_2\,x_{21} \\ c_3\,\dot{x}_1 \end{bmatrix} \qquad \mathbf{w} = \begin{bmatrix} \omega_1 \\ \omega_2 \\ \omega_3 \end{bmatrix} \quad (12)$$

The composition of the matrices of the generalized plant are detailed in Eq.13. The following assumptions are made on the generalized plant for a direct application of the DGKF design procedure of H_∞ controllers:

- $(-\mathbf{A},\ \mathbf{B}_1)$ is stabilizable and $(\mathbf{C}_1,\ -\mathbf{A})$ is detectable.
- $(-\mathbf{A},\ \mathbf{B}_2)$ is stabilizable and $(\mathbf{C}_2,\ -\mathbf{A})$ is detectable.
- $\mathbf{D}_{11} = \mathbf{O}$ and $\mathbf{D}_{22} = \mathbf{O}$
- $\mathbf{D}_{21}^T\,[\,\mathbf{C}_2 \quad \mathbf{D}_{21}\,] = [\,\mathbf{O} \quad \mathbf{I}\,]$.
- $\begin{bmatrix} \mathbf{B}_2 \\ \mathbf{D}_{12} \end{bmatrix} \mathbf{D}_{12}^T = \begin{bmatrix} \mathbf{O} \\ \mathbf{I} \end{bmatrix}$

A detailed description of the generalized plant with input vectors $\mathbf{w}$ and $\mathbf{u}$ and output vectors $\mathbf{z}$ and $\mathbf{y}$ is shown in Fig.3.

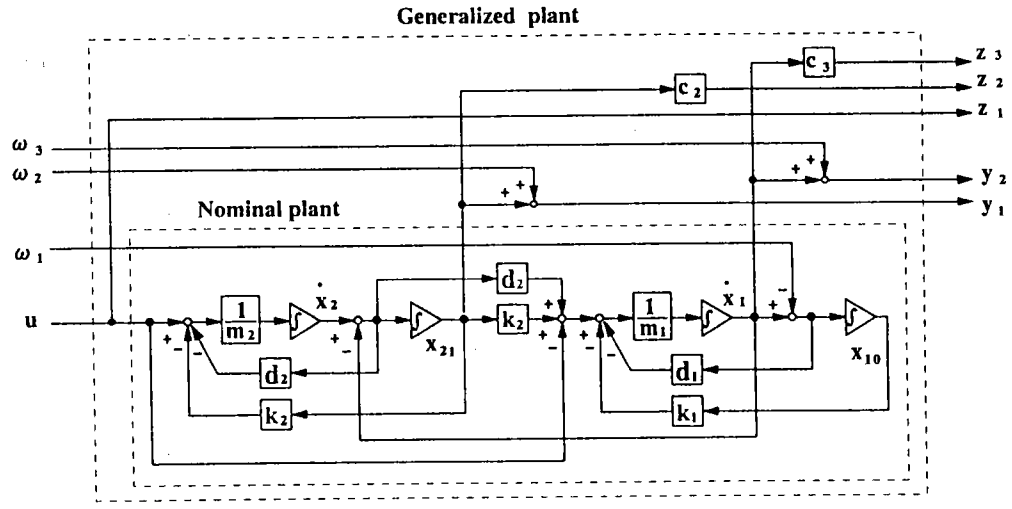

Figure 3: Block diagram of generalized plant

$$\begin{bmatrix} \ddot{x}_2 \\ \dot{x}_{21} \\ \ddot{x}_1 \\ \dot{x}_{10} \\ \hline y_1 \\ y_2 \\ \hline z_1 \\ z_2 \\ z_3 \end{bmatrix} = \left[\begin{array}{cccc|c|cccc} -d_2/m_2 & -k_2/m_2 & d_2/m_2 & 0 & 1/m_2 & 0 & 0 & 0 \\ 1 & 0 & -1 & 0 & 0 & 0 & 0 & 0 \\ d_2/m_1 & k_2/m_1 & -(d_1+d_2)/m_1 & -k_1/m_1 & -1/m_1 & d_1/m_1 & 0 & 0 \\ 0 & 0 & 1 & 0 & 0 & -1 & 0 & 0 \\ \hline 0 & 1 & 0 & 0 & 0 & 0 & 1 & 0 \\ 0 & 0 & 1 & 0 & 0 & 0 & 0 & 1 \\ \hline 0 & 0 & 0 & 0 & 1 & 0 & 0 & 0 \\ 0 & c_2 & 0 & 0 & 0 & 0 & 0 & 0 \\ 0 & 0 & c_3 & 0 & 0 & 0 & 0 & 0 \end{array}\right] \begin{bmatrix} \dot{x}_2 \\ x_{21} \\ \dot{x}_1 \\ x_{10} \\ \hline u \\ \hline \omega_1 \\ \omega_2 \\ \omega_3 \end{bmatrix} := \left[\begin{array}{c|c|c} -A & B_1 & B_2 \\ \hline C_1 & D_{11} & D_{12} \\ \hline C_2 & D_{21} & D_{22} \end{array}\right] \begin{bmatrix} \dot{x}_2 \\ x_{21} \\ \dot{x}_1 \\ x_{10} \\ \hline u \\ \hline \omega_1 \\ \omega_2 \\ \omega_3 \end{bmatrix} \quad (13)$$

4 H_∞ Robust Control

As it was mentioned in the previous section, the objective of the control system is to minimize the value of the performance variables in order to improve the vibration isolation properties of the building. Since there are several performance variables, the objective of the control system will be to minimize the norm of the perfomance vector **z**. In optimal control theory, two are the most common performance measures of vector **z**: H_2 norm and H_∞ norm. The H_2 norm is related to the linear quadratic Gaussian (LQG) optimal control problem. The H_∞ norm is usually defined in the frequency-domain for a stable transfer matrix and is the performace measure to be optimized when designing controllers according to H_∞ robust control theory.

H_∞ controllers minimize the H_∞ norm of the transfer function $\mathbf{T}_{zw}$ from disturbance **w** to controlled output vector **z**. The H_∞ norm of a transfer function is defined as its maximum singular value σ_{max} over all the frequency spectrum:

$$\|\mathbf{T}_{zw}\|_\infty = \sup_\omega \sigma_{max}[\mathbf{T}_{zw}(j\omega)] \quad (13)$$

Optimal (sub-optimal) H_∞ controllers are designed so that the following condition is satisfied:

$$\|\gamma\, \mathbf{T}_{zw}\|_\infty < 1 \quad (14)$$

where γ is the maximum possible scalar value. The H_∞ controller can be structured from the positive semi-definite solutions **X** and **Y** of the following two Riccati equations:

$$\mathbf{X}[\mathbf{B}_1\mathbf{B}_1^T - \gamma^2\mathbf{B}_2\mathbf{B}_2^T]\mathbf{X} + \mathbf{A}^T\mathbf{X} + \mathbf{X}\mathbf{A} - \mathbf{C}_2^T\mathbf{C}_2 = \mathbf{O} \quad (15)$$

$$\mathbf{Y}[\mathbf{C}_1^T\mathbf{C}_1 - \gamma^2\mathbf{C}_2^T\mathbf{C}_2]\mathbf{Y} + \mathbf{A}\mathbf{Y} + \mathbf{Y}\mathbf{A}^T - \mathbf{B}_2\mathbf{B}_2^T = \mathbf{O} \quad (16)$$

In order to design an internally stable H_∞ controller, the spectral radius (maximum absolute eigenvalue) of the product **XY** should satisfy the following inequality:

$$\gamma^2\rho(\mathbf{X}\mathbf{Y}) < 1 \quad (17)$$

The H_∞ controller is described by the following state-space equation:

$$\dot{\hat{\mathbf{x}}} = -\hat{\mathbf{A}}\hat{\mathbf{x}} + \hat{\mathbf{B}}_2\mathbf{y} \quad (18)$$

$$u = -\hat{\mathbf{C}}_2\hat{\mathbf{x}} \quad (19)$$

where:

$$\hat{\mathbf{A}} = \mathbf{A} + [\mathbf{B}_1\mathbf{B}_1^T - \gamma^2\mathbf{B}_2\mathbf{B}_2^T]\mathbf{X} + \mathbf{Z}\mathbf{Y}\mathbf{C}_1^T\mathbf{C}_1 \quad (20)$$

$$\hat{\mathbf{B}}_2 = \mathbf{Z}\mathbf{Y}\mathbf{C}_1^T \quad (21)$$

$$\hat{\mathbf{C}}_2 = \mathbf{B}_1^T\mathbf{X} \quad (22)$$

and

$$\mathbf{Z} = (\mathbf{I} - \gamma^2\mathbf{Y}\mathbf{X})^{-1} \quad (23)$$

H_∞ controllers have the separation structure of observer-based compensators: the controller is composed of an observer and a feedbak gain which corresponds to the optimal feedback gain for the case of full state feedback. The state vector of the H_∞ observer, $\hat{\mathbf{x}}$, is the H_∞ estimation of the state vector **x** of the generalized plant. Figure 4 shows the

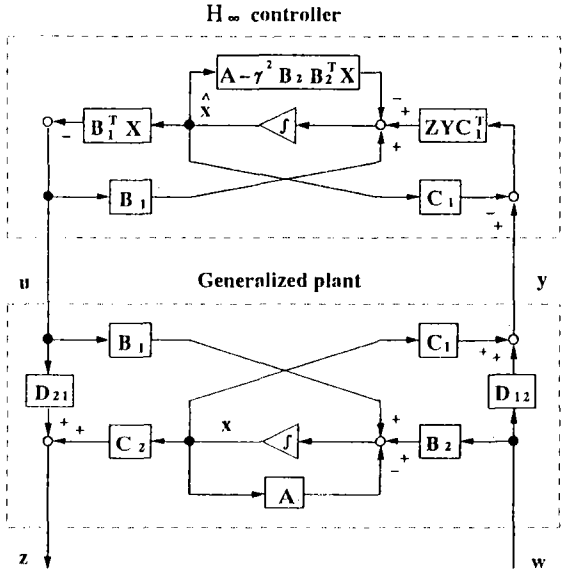

Figure 4: Structure of generalized plant and H_∞ controller

block diagram of the generalized plant and H_∞ controller where it can be noted that the internal structure of the H_∞ controller is similar to that of the generalized plant.

H_2 optimal controllers can be designed according to the same procedure described above with the only difference being the value assigned to γ: while optimal H_∞ controllers are designed for the maximum possible value of γ, optimal H_2 controllers are designed considering $\gamma = 0$ which can be interpreted as the fact that H_2 controllers are designed without imposing any constraint on the H_∞ norm of the tranfer function $\mathbf{T}_{zw}$.

5 Results and Analysis

After H_∞ and H_2 controllers were designed, their properties and performance were analyzed in the time and frequency domains. In the following, the root-locus, frequency and step responses of the closed-loop system will be analyzed. Also the estimation capabilities of H_∞ and H_2 observers and the robustness properties of the H_∞ and H_2 controllers will be examined.
The baseline parameters of the building model correspond to a laboratory-scale experimental set-up which is in construction. The list of parameters is shown in Table 1.

5.1 Root-locus on S-plane

Figure 5 shows the root-locus plot of the closed-loop system with controllers designed with different values of γ. Since the state dimension of the building and controller is 4 (for each one), the closed loop systems has 8 poles. As noted in the figure, the 4 poles related to the controller change as γ varies from $\gamma = 0$ to $\gamma_{max} = 0.00071428$. As it was mentioned in Section 4, $\gamma = 0$ corresponds to the optimal H_2 controller and $\gamma = \gamma_{max}$ corresponds to the optimal H_∞ controller.
It is important to note that as γ varies from 0 to γ_{max}, the poles of the closed-loop system move to the left on the

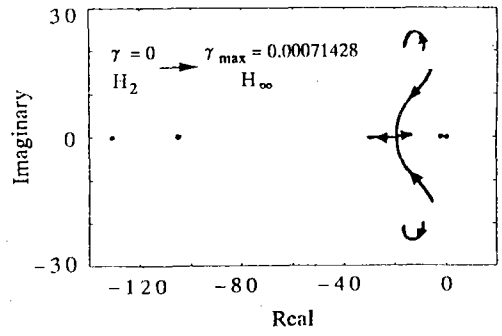

Figure 5: Root-locus of closed-loop poles

S-plane. It is known that as the poles move to the left the stability and speed of response of the closed-loop system are improved.

5.2 Frequency response

Figure 6 shows the gain of the frequency response of the building mass acceleration $\ddot{x}_1$ and relative displacement x_{10} and the relative displacement of the vibrating mass x_{21} for the system with H_∞ control, H_2 control and passive system (no control). It can be noted that the peak of the response around the resonant frequency has been significantly reduced by both H_∞ and H_2 control. From the response of x_{10} it can be noted that the system with H_∞ control presents better vibration isolation properties than the system with H_2 control.
The gain of the frequency response of x_{21} is higher for H_∞ control than for H_2 control and both responses are higher than the response of the passive system. This behavior is expected since the objective of the control system is to absorbe the vibrational motion coming from ground isolating the building with the motion of the vibrating mass m_2 of the control system.

5.3 Step response

Figure 7 compares the step responses of the performance variables $\ddot{x}_1$, x_{10} and x_{21} for active H_∞, active H_2 and passive system. Similarly as the frequency responses shown before, the step responses of $\ddot{x}_1$ and x_{10} for H_∞ and H_2 control are better than the response of the passive system: the rising and settling times of $\ddot{x}_1$ and the overshoot and settling time of x_{10} are significantly improved by active control. This improvements are more significative for H_∞ control than for H_2 control. The relative displacement x_{21} of the vibrating mass m_2 is higher for H_∞ control than for H_2 control and for the passive system as was for the frequency response.

5.4 Response of H_∞ and H_2 observers

Figure 8 and 9 compare the time history of state variables $\dot{x}_1$ and x_{10} of the actual system with the estimated variables $\hat{\dot{x}}_1$ and $\hat{x}_{10}$ of the H_∞ and H_2 observers when the building is excited by stochastic motion of ground simulating and earthquake. From these responses it can be noted

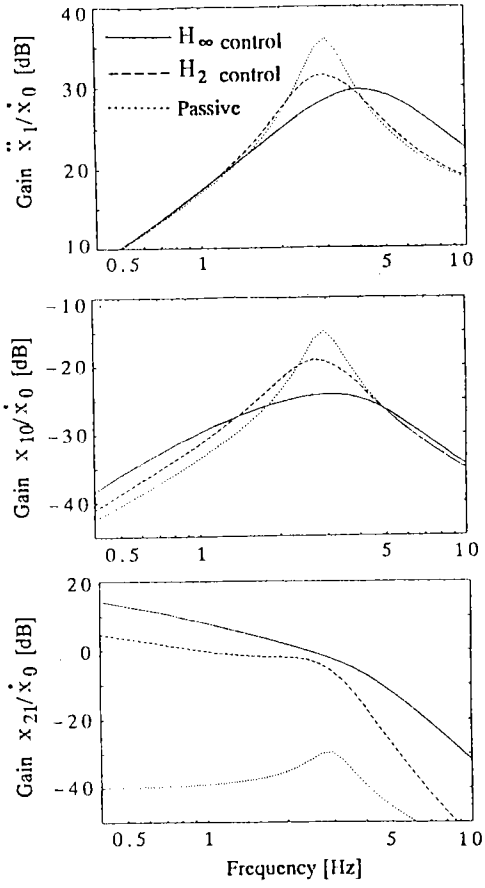

Figure 6: Frequency response for H_∞ control, H_2 control and passive system

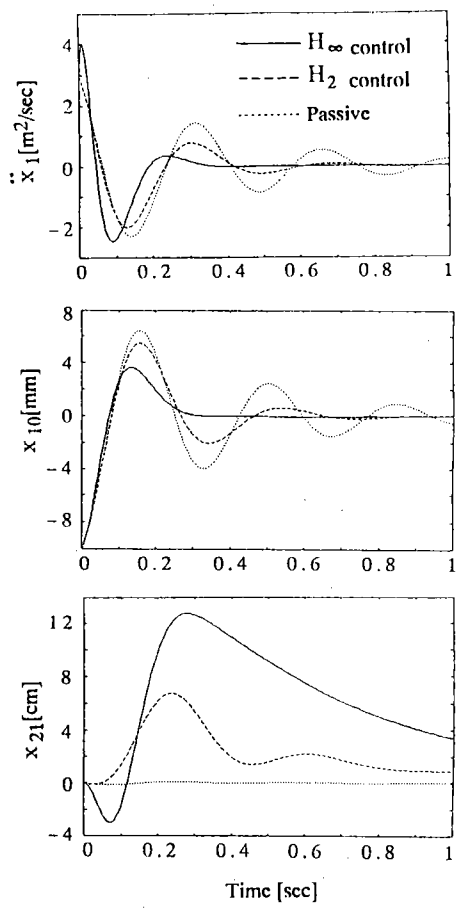

Figure 7: Step response for H_∞ control, H_2 control and passive system

that the H_∞ observer (Fig.8) estimate the actual state variables much better than the H_2 observer (Fig.9). The better estimation capabilities of the H_∞ observer in part explains the better performance of the H_∞ controller.

5.5 Change of nominal parameters

In order to examine the robustness properties of H_∞ and H_2 controllers against parameter variations, the response of the system for modified values of the parameters have been analyzed. Figure 10 compares the step response of the system with H_∞ and H_2 controllers when the nominal mass of the building has been incremented by 30%. It can be noted that the responses for H_∞ control have faster rising and settling times. For x_{10} it can be noted that the overshoot is lesser for H_∞ control than for H_2 control.
Similar responses are obtained when the equivalent damping of the building is reduced in 30% as shown in Fig.11. While the vibrational motion of the building with H_∞ is fastly damped out, it remains a longer time in the system with H_2 control.

6 Conclusions

This paper has presented a procedure for the modeling and design of the vibration control system of high-rise

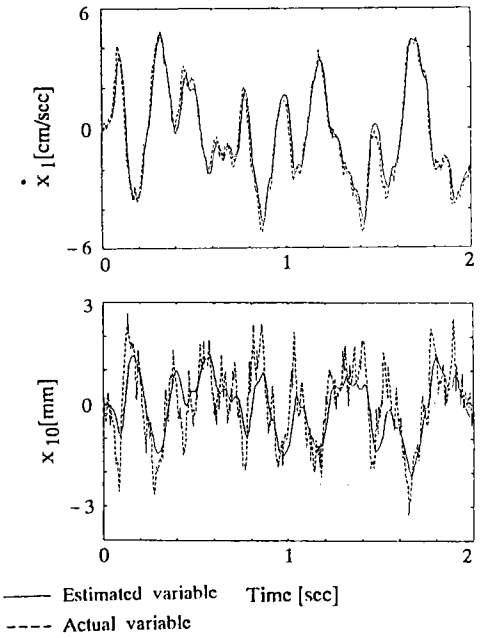

Figure 8: State estimation with H_∞ observer

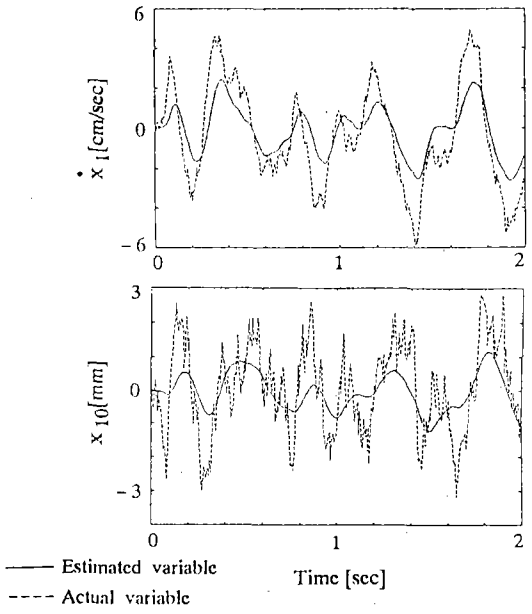

Figure 9: State estimation with H_2 observer

buildings. The design procedure of H_2 and H_∞ controllers have been detailed and the performance of the building with H_∞ and H_2 control have been analyzed and compared. It has been found that the building with H_∞ control presents better vibration isolation properties than the building with H_2 control. The estimation capabilities of H_∞ and H_2 observers have been analyzed and it was found that H_∞ observers can identify the state vector of the actual system much better than H_2 observers. The robustness properties of H_∞ and H_2 controllers against parameter variations were analyzed and it was found that the H_∞ controller presents better robustness properties.
Finally it is important to say that the performance improvements and robustness achieved with H_∞ control are at the expense of larger actuator forces.

7 References

[1] Okada R., Takahashi Y., and Hayase M., 'Compensator Design of a Servo-System Using H_∞ Control', (in Japanese), Proc. of SICE'93, pp.85-88.
[2] Doyle J.C., Glover K., Khargonekar P., and Francis B., 'State-Space Solutions to Standard H_2 and H_∞ Control Problems', IEEE Trans. on Automatic Control, Vol.34., No.8, pp.831-847, 1989.
[3] Stoorvogel A., 'The H_∞ Control Problem. State-Space Approach', Prentice Hall International, 1992.

Table 1. List of Parameters of Building Model

Building equivalent mass	m_1	10.0 Kg
Building equivalent stiffness	k_1	3552.0 N/m
Building equivalent damping	d_1	57.0 N.s/m
Controller body vibrating mass	m_1	0.5 Kg
Controller body equivalent stiffness	k_1	0.0 N/m
Controller body equivalent damping	d_1	50.0 N.s/m
Weighting coefficient c_2	c_2	100
Weighting coefficient c_3	c_3	800

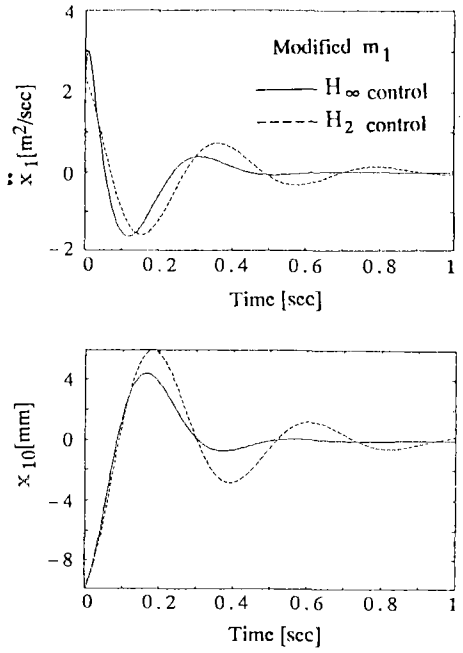

Figure 10: Step response for modified mass m_1 (increased 30%)

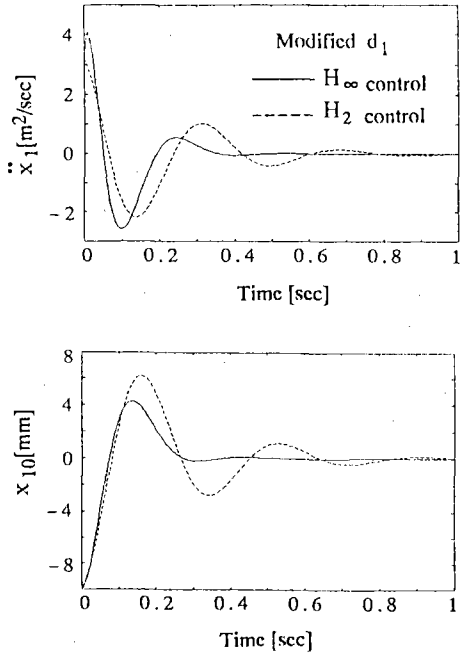

Figure 11: Step response for modified damping d_1 (decreased 30%)